ACCSCIENCE PUBLISHING

Gene & Protein in Disease

ORIGINAL RESEARCH ARTICLE

Unraveling the mechanism of Si-Ni-San against non-alcoholic fatty liver disease: An integration of network pharmacology and experimental verification

Yue Hu, Bowen Yang, Yishu Wang, Chengyao Xiao, Tingting Wang, Cancan Guo, Yunfei Li, and Jingxia Du*

Department of Pharmacy, College of Basic Medicine and Forensic Medicine, Henan University of Science and Technology, Luoyang, Henan, China

Abstract

The global prevalence of non-alcoholic fatty liver disease (NAFLD) is rising. Si-Ni-San (SNS), a classical herbal formula for chronic liver disease, has unclear mechanisms against NAFLD. This study integrated network pharmacology with in *vivo* validation to investigate its mechanisms. Potential SNS and NAFLD targets were retrieved from public databases. A protein-protein interaction network was identified, followed by Gene Ontology (GO) functional enrichment analysis and Kyoto Encyclopedia of Genes and Genomes (KEGG) pathway enrichment analysis. For *in vivo* experiments, NAFLD was induced in mice by feeding a high-fat diet, with SNS administered orally for therapeutic intervention. Liver Oil Red O staining was evaluated, and biochemical parameters, including total cholesterol (TC) and triglyceride (TG) in serum, were assessed. Furthermore, molecular techniques were used to examine the expression levels of inflammatory and oxidative stress-related factors predicted by network pharmacology. A total of 157 overlapping potential targets between SNS and NAFLD were identified, yielding the top 10 hub targets including IL-6, TNF-α, HIF-1α, MMP-9, AKT1, STAT3, Caspase-3, JUN, PTGS2, and TGF-β1. Additional oxidative stress-related targets (NRF2, HO-1, NQO1) were also examined. KEGG/GO analyses indicated involvement of inflammation and oxidative stress pathways. Molecular docking further demonstrated strong binding affinities of its active components with STAT3 and NRF2. *In vivo*, SNS reduced liver weight index, lipid droplets, serum TC, and TG levels. Western blot analysis showed that SNS treatment led to a marked inhibition of JAK2 and STAT3 phosphorylation. SNS downregulated the expression of pro-inflammatory cytokines, such as *Il6* and *Il1b*, while upregulating endogenous antioxidant proteins Sestrin2 and NRF2, thereby enhancing the expression of key downstream antioxidant genes, including *Nqo1* and *Hmox1*. In conclusion, integrated network pharmacology and *in vivo* validation demonstrated that SNS ameliorates NAFLD by activating the Sestrin2/NRF2/HO-1 pathway to enhance antioxidant capacity and inhibiting the JAK2/STAT3 pathway to alleviate inflammatory injury.

Keywords: Si-Ni-San; Non-alcoholic fatty liver disease; Network pharmacology analysis; JAK2/STAT3; Sestrin2/NRF2/HO-1

***Corresponding author:**
Jingxia Du
(9902388@haust.edu.cn)

Citation: Hu Y, Yang B, Wang Y, *et al*. Unraveling the mechanism of Si-Ni-San against non-alcoholic fatty liver disease: An integration of network pharmacology and experimental verification. *Gene Protein Dis.*
doi: 10.36922/GPD026030002

Received: January 15, 2026

Revised: April 24, 2026

Accepted: April 30, 2026

Published online: May 28, 2026

Copyright: © 2026 Author(s). This is an Open-Access article distributed under the terms of the Creative Commons Attribution License, permitting distribution, and reproduction in any medium, provided the original work is properly cited.

Publisher's Note: AccScience Publishing remains neutral with regard to jurisdictional claims in published maps and institutional affiliations.

1. Introduction

Globally, non-alcoholic fatty liver disease (NAFLD) represents a highly prevalent chronic hepatic disorder, with a global prevalence of up to 25%.[1] NAFLD represents a disease continuum, beginning with fat accumulation (steatosis) and advancing to inflammatory non-alcoholic steatohepatitis (NASH).[2] With disease progression, NASH may evolve into progressive liver fibrosis, ultimately culminating in cirrhosis and hepatocellular carcinoma.[3] The pathogenesis of NAFLD involves multiple metabolic dysregulations and oxidative stress responses,[4] wherein interconnected pathological processes, including mitochondrial dysfunction, aberrant lipid metabolism, and endoplasmic reticulum stress, collectively drive disease progression.[5,6] Notably, immune cell-mediated inflammation serves as a pivotal mechanism driving the transition from fatty liver to the more severe condition of NASH.[7]

As obesity rates continue to climb globally, the incidence of NAFLD is showing a rapid increase parallel to the obesity epidemic.[8,9] However, there are no approved targeted therapeutic agents, and there is a significant unmet need for clinical management.[10] In this context, traditional Chinese medicine (TCM) formulations exhibit distinctive therapeutic advantages attributable to their characteristic multi-target and multi-pathway regulatory properties. Si-Ni-San (SNS) is a classic TCM formula composed of bupleurum (Chaihu), white peony root (Baishao), immature bitter orange (Zhishi), and licorice (Gancao). It is primarily used to disperse liver stagnation and relieve symptoms associated with liver qi depression.[11] The pathogenesis of NAFLD is closely linked to metabolic disturbances such as insulin resistance. From the perspective of TCM, liver qi depression can lead to the impeded flow of qi and blood, resulting in metabolic dysregulation.[12] Nonetheless, the contemporary scientific understanding of the mechanisms underlying its therapeutic effects, especially concerning its systemic regulation of the pathogenesis of NAFLD, remains insufficiently elucidated.[11,13]

Network pharmacology and molecular docking analysis have been demonstrated to be effective approaches for elucidating the molecular mechanisms of TCM.[14] Current research has shown that TCM can restore systemic homeostasis by modulating metabolic disorders and inflammatory responses, which are highly compatible with the pathological features of NAFLD.[13] The potential mechanisms of SNS may involve modulation of core pathological processes, including lipid accumulation, oxidative stress, and inflammatory mediators,[15] while also influencing regulatory factors such as SIRT2 to alleviate endoplasmic reticulum stress and inflammatory responses.[16] Emerging studies have revealed that certain TCM monomers, such as saponin D, exert anti-steatotic effects by modulating lipid metabolism-related pathways,[17] which provides critical insights for elucidating the mechanistic basis of SNS.

The JAK2/STAT3 signaling pathway is an evolutionarily conserved transmembrane signal transduction cascade that mediates cellular responses to diverse cytokines, interferons, and growth factors.[18,19] JAK2 undergoes autophosphorylation and subsequently phosphorylates STAT3, and then the phosphorylated STAT3 dimerizes and translocates to the nucleus, where it functions as a transcription factor to regulate the expression of downstream target genes, such as *VEGFA* and *CCND*.[20–22] The JAK2/STAT3 signaling pathway, a pivotal regulator of inflammation and cellular proliferation, has a dual role in hepatic pathologies, facilitating tissue repair while also contributing to inflammation and fibrosis. Notch1 deficiency inhibits JAK2/STAT3 phosphorylation, impairing thrombopoietin production in hepatocytes and compromising liver regeneration and repair.[23] In inflammatory settings, JAK2/STAT3 activation induces pro-inflammatory cytokine release and macrophage polarization, exacerbating chronic liver disease progression.[24]

Sestrin2, a stress-inducible protein, plays a key role in cytoprotection and antioxidant defense by activating the NRF2 signaling pathway. Sestrin2 has been shown to mitigate ferroptosis through the KEAP1/NRF2 signaling pathway, which is closely associated with NRF2-mediated attenuation of oxidative stress.[25] In NAFLD, Sestrin2 modulates inflammation and lipid metabolism, with its dysregulated expression linked to disease progression.[26] NRF2 serves as a master regulator in chronic liver diseases, counteracting oxidative stress to exert protective effects. However, its function is highly contingent on the specific context. For instance, NRF2/HO-1 activation reduces oxidative stress and inflammation in alcoholic liver injury,[27] while it may exacerbate liver damage in cholestatic conditions, highlighting the complexity of its pathological implications.[28] HO-1, as the downstream of NRF2, promotes hepatoprotection by interacting with STAT3. This is exemplified in ischemia–reperfusion injury models, in which STAT3 activation mitigates hepatic damage by modulating metabolic pathways associated with HO-1.[29] In summary, the Sestrin2/NRF2/HO-1 and JAK2/STAT3 pathways form a complex signaling network that coordinately regulates oxidative stress, inflammatory responses, and metabolic homeostasis.

This study aims to systematically elucidate the active components, potential targets, and molecular mechanisms

of SNS against NAFLD through an integrated approach combining network pharmacology prediction with experimental validation.

2. Materials and methods

2.1. Network pharmacology analysis

The component targets of Chaihu (Bupleuri radix), Gancao (Glycyrrhizae radix et rhizoma), Baishao (*Paeonia mairei* H. Lév.), and Zhishi (Aurantii fructus immaturus) were retrieved from the TCM Systematic Pharmacology Database (TCMSP) (https://www.tcmsp-e.com/tcmsp.php). Preliminary screening was performed with the parameters set at oral bioavailability ≥ 30% and drug-likeness ≥ 0.18. After removing duplicates, the key targets of the main active components of SNS were obtained. Subsequently, using GeneCards (https://www.genecards.org/), OMIM (https://www.omim.org/), and TTD (https://db.idrblab.net/ttd/), the keywords "NAFLD" and "non-alcoholic fatty liver disease" were entered for retrieval. After consolidating the results and removing duplicate genes, the target genes associated with NAFLD were obtained. The key targets of SNS and the target genes of NAFLD were intersected, and a Venn diagram was constructed. The overlapping targets represent the potential therapeutic targets of SNS in the intervention of NAFLD. Using Cytoscape 3.8.2 software, the "TCM–active ingredient–target–disease" network was constructed, and core components were identified based on degree, betweenness centrality, and closeness centrality. The selected targets were imported into the Search Tool for the Retrieval of Interacting Genes/Proteins (STRING) database to build a protein–protein interaction (PPI) network between SNS and NAFLD. The maximal clique centrality algorithm then identified the 10 most crucial targets. In addition, enrichment analyses for Gene Ontology (GO) terms and Kyoto Encyclopedia of Genes and Genomes (KEGG) pathways were conducted using the clusterProfiler package in R. The analysis was conducted with a significance threshold of corrected $p < 0.05$, followed by sorting the results in ascending order by p-value. The top five active components were selected for molecular docking with STAT3 and NRF2. The three-dimensional (3D) structures of target proteins and bioactive compounds were obtained from the Research Collaboratory for Structural Bioinformatics Protein Data Bank and PubChem databases. Protein preparation (including water removal, hydrogen addition, and heteroatom deletion) was performed using PyMOL, followed by molecular docking with AutoDock.

2.2. Extraction of Si-Ni-San

The investigated formulation, composed of Chaihu, Zhishi, Baishao, and Gancao in a 1:1:1:1 ratio, was purchased from Luoyang Zhang ZhongJing Traditional Chinese Medicine Pharmacy (China). The combined herbs were soaked in water for 0.5 h, then decocted with 10 volumes of water for 2 h. The resulting decoction was filtered and concentrated to 1 g/mL. For subsequent experiments, the final extract was refrigerated at 4 °C.

2.3. Animal experiments

A total of 27 male C57BL/6 mice (age, 4–5 weeks, 15 ± 2 g) were supplied by the institutional Experimental Animal Center (Tongji Medical College, License No. SCXK 20190008). All mice were housed in a controlled environment with relatively stable temperature (22 ± 2 °C) and humidity (50 ± 5%). Following a seven-day acclimatization under a 12-h light/dark cycle, the mice were randomized into three groups: normal-fat diet (NFD, 10% kcal fat), high-fat diet (HFD, 60% kcal fat), and high-fat diet plus SNS (HFD + SNS) (n = 9 per group). After feeding with NFD or HFD for 8 consecutive weeks, mice in both NFD and HFD groups received daily oral gavage of normal saline. The HFD + SNS group was administered SNS decoction (10 mL/kg/day) via oral gavage concurrently with high-fat feeding for eight consecutive weeks, with all groups having *ad libitum* access to food and water. At the experimental endpoint, mice were anesthetized by intraperitoneal injection of 1% sodium pentobarbital, followed by blood collection via retro-orbital venous plexus puncture and subsequent liver tissue harvesting for analysis.

The animal experiments were approved by the Institutional Animal Care and Use Committee of Henan University of Science and Technology (Luoyang, China) and were conducted in strict accordance with the National Institutes of Health (NIH) guidelines for the care and use of laboratory animals.

2.4. Liver index analysis

At the end of the animal experiment, mice from all groups were anesthetized by intraperitoneal injection of 1% sodium pentobarbital. Subsequent to excision, the livers were weighed. The liver index was calculated as the ratio of liver weight to body weight (liver weight/body weight).

2.5. Determination of serum biochemical parameters

Blood was collected from anesthetized mice via the retro-orbital plexus. Following a 2-h clotting period at room temperature (22–24 °C), the samples were subsequently centrifuged at 4 °C and 3,000 rpm for 20 min to isolate serum. Serum was analyzed for total cholesterol (TC) and triglycerides (TG) using commercial kits according to the manufacturer's guidelines (Nanjing Jiancheng Bioengineering Institute, China).

2.6. Oil Red O staining

Fresh liver tissue was fixed with 4% paraformaldehyde. Following dehydration and immersion in sucrose solution, the tissue was embedded in optimal cutting temperature compound (OCT) and subsequently rapidly frozen at −80 °C for 72 h. The slices were cut on a freezing microtome (Model MNT, REF #10160000, SLEE Medical GmbH, Germany) at 5 μm, mounted onto slides, and air-dried at room temperature. The sections were gently rinsed with phosphate-buffered saline to remove residual OCT compound. Filtered Oil Red O working solution was applied to cover the tissue sections, followed by incubation in the dark at room temperature for 10 min. Subsequently, the sections were briefly differentiated in 60% isopropanol for 30 s, rinsed thoroughly with distilled water, and counterstained with hematoxylin for approximately 1 min. Finally, the slides were coverslipped with glycerol–gelatin and imaged under a light microscope (Model BX53, Olympus Corporation, Japan).

2.7. RNA extraction and quantitative real-time polymerase chain reaction

Approximately 30 mg of liver tissue was immediately placed in liquid nitrogen for rapid freezing, then homogenized using a tissue homogenizer (Model JY92-II, Ningbo Scientz Biotechnology Co., Ltd., China). RNA was extracted using the TRIzol reagent (CWBio, China) according to the manufacturer's protocol. RNA purity and concentration were determined by measuring the absorbance ratio at 260/280 nm (Nanodrop ONE, Thermo Fisher Scientific, United States of America [USA]), ensuring a ratio of 1.8–2.0. The RNA was then reverse-transcribed into cDNA by using the HiScript II Reverse Transcriptase Kit (CWBio, China). Quantitative real-time polymerase chain reaction (qPCR) was performed using SYBR Green PCR Master Mix (CWBio, China), according to the manufacturer's protocols. The mRNA expression of specific inflammatory factors and oxidative stress markers was quantified. The qPCR was performed using the 7500 Real-Time PCR System (Applied Biosystems, Life Technologies Holdings Pte Ltd, Singapore) with the following conditions: 30 s of pre-denaturation at 95 °C, 10 s of denaturation at 95 °C, and 30 s of annealing and extension at 60 °C, for a total of 40 cycles. The relative expression levels of the target genes were calculated by the Ct method ($2^{-\Delta\Delta Ct}$), with *Actb* as the internal reference gene. The primer sequences are listed in Table 1.

2.8 Western blot analysis

Following protein extraction with RIPA lysis buffer (Solarbio, China), total protein concentration was measured. Equivalent protein amounts were resolved by SDS–PAGE and electro-transferred onto polyvinylidene fluoride membranes (Millipore, USA).The membranes were blocked for 1 h in tris-buffered saline with Tween 20 (TBST; Solarbio, China) containing 5% BSA and then incubated overnight at 4 °C with primary antibodies diluted in the same blocking solution. Following three washes with TBST, the membranes were incubated with a horseradish peroxidase (HRP)-conjugated secondary antibody (diluted 1:5,000; Proteintech, China) for 1 h. Finally, immunoreactive bands were detected using an enhanced chemiluminescence system (Model Tanon-4600, Tanon Science Technology Co., Ltd., China). The following primary antibodies were used: NRF2 (1:500; 805931AP, Proteintech, China), Sestrin2 (1:3000; 107951AP, Proteintech, China), HO-1 (1:3000; 107011AP, Proteintech, China), JAK2 (1:1000; 3230S, Cell Signaling Technology, USA), phospho-JAK2 (1:1000; 3774S, Cell Signaling Technology, USA), STAT3 (1:1000; 12640S, Cell Signaling Technology, USA), phospho-STAT3 (1:1000; 9145S, Cell Signaling Technology, USA), and GAPDH (1:10000; Sangon Biotech, China). GAPDH was used as an internal loading control, and band intensities were quantified with ImageJ software (version 1.80).

Table 1. Sequences of reverse transcriptase-quantitative polymerase chain reaction primer

Gene	Sequence（5'–3'）
Il6	Forward: TTCTTGGGACTGATGCTGGTGAC
	Reverse: GTGGTATCCTCTGTGAAGTCTCCTC
Il1b	Forward: CTCGCAGCAGCACATCAACAAG '
	Reverse: CCACGGGAAAGACACAGGTAGC
Tnf	Forward: ACGCTCTTCTGTCTACTGAACTTCG
	Reverse: TGGTTTGTGAGTGTGAGGGTCTG '
Nqo1	Forward: GCGAGAAGAGCCCTGATTGTACTG
	Reverse: AGCCTCTACAGCAGCCTCCTTC
Hmox1	Forward: ACCGCCTTCCTGCTCAACATTG
	Reverse: CTCTGACGAAGTGACGCCATCTG
Actb	Forward: GGAGATCACAGCTCTGGCT
	Reverse: GTCGATTGTCGTCCTGAGG

2.9 Statistical analysis

All experimental data, excluding those derived from network pharmacology analyses involving specialized algorithms, are expressed as means ± standard error of the mean. Data analysis and graphical visualization were performed using GraphPad Prism 9.0. For comparisons across multiple groups within a single experimental condition, a one-way analysis of variance was used, with $p < 0.05$ as the criterion for statistical significance.

3. Results

3.1. Key bioactive compounds in Si-Ni-San and target-disease relationships

The active components of Chaihu, Baishao, Zhishi, and Gancao were retrieved from the TCMSP database. The top 10 compounds ranked by degree value were identified as the primary bioactive constituents potentially responsible for treating NAFLD (Table 2). A total of 2,798 NAFLD-related disease targets were collected from the GeneCards, OMIM, and TTD databases. After removing duplicates using the Venny platform, 157 overlapping targets between the active components of SNS and NAFLD-related targets were identified (Figure 1A). An interaction network was constructed with Cytoscape 3.8.2 to visualize the relationships between the four key herbal components of SNS and the 157 shared NAFLD targets (Figure 1B). Within this network, compounds such as MOL000098 (quercetin), MOL000422 (kaempferol), and MOL000006 (luteolin) had the highest number of connections, suggesting a potential central role in the SNS mechanism against NAFLD.

3.2. Integrated bioinformatics analysis of Si-Ni-San for non-alcoholic fatty liver disease treatment: Protein–protein interaction network construction, Gene Ontology, and Kyoto Encyclopedia of Genes and Genomes enrichment

The 157 overlapping target genes shared by the active components of SNS and NAFLD-related targets were imported into the STRING database to establish a high-confidence PPI network (Figure 2A). In this network, nodes represent target proteins, and edges represent functional interactions between them. The resulting PPI network comprises 153 nodes and 3,326 edges, with nodes of higher connectivity indicative of greater functional significance within the network. As illustrated in Figure 2B, the top 10 hub targets were identified as IL-6, TNF, HIF-1α, MMP-9, AKT1, STAT3, Caspase-3, JUN, PTGS2, and TGF-β1, based on degree values.

Subsequently, GO and KEGG enrichment analyses were performed using the ClusterProfiler package in R. GO enrichment yielded 2,374 biological processes, 70 cellular components, and 161 molecular functions. After filtering by p-value ($p < 0.05$), the top 10 terms in each category were visualized (Figure 2C). These were significantly associated with lipid metabolism regulation, oxidative stress, the inflammatory response, insulin resistance, membrane rafts, membrane microdomains, nuclear receptor activity, and lipid binding. KEGG pathway analysis revealed 181 pathways enriched at a highly significant level ($p < 0.05$), among which the top 20 included PI3K-AKT, MAPK, TNF, NAFLD, NF-κB, and oxidative stress-related pathways (Figure 2D). These findings indicate that SNS may exert multi-target therapeutic effects on NAFLD by coordinating the modulation of interconnected biological processes.

Overall, the network pharmacology analysis suggests that SNS alleviates NAFLD pathogenesis via its bioactive components by simultaneously targeting lipid dysregulation, inflammatory activation, oxidative stress, and metabolic dysfunction.

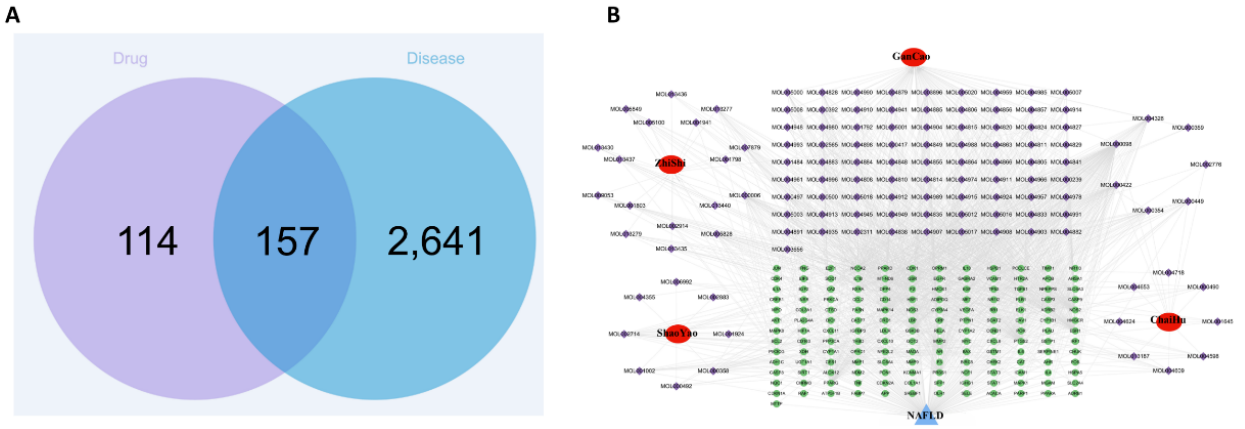


Figure 1. Construction of the Si-Ni-San–component–target–non-alcoholic fatty liver disease (NAFLD) network. (A) Venn diagram illustrating the overlapping targets between drug-related and NAFLD-related genes. (B) Network diagram depicting interactions among drugs, diseases, and targets.

Table 2. The top 10 active components in Si-Ni-San

Traditional Chinese medicine	Molecule name	MOL ID	Degree	Betweenness centrality	Closeness centrality
Chaihu, Gancao	Quercetin	MOL000098	105	0.161845	0.547389
Chaihu, Shaoyao	Kaempferol	MOL000422	44	0.036466	0.442879
Zhishi	Luteolin	MOL000006	40	0.026735	0.436055
Zhishi, Gancao	Naringenin	MOL004328	28	0.021025	0.414348
Zhishi	Nobiletin	MOL005828	24	0.013567	0.415565
Shaoyao	Baicalein	MOL002714	22	0.010147	0.411936
Gancao	7-Methoxy-2-methyl isoflavone	MOL003896	22	0.006379	0.411936
Gancao	Formononetin	MOL000392	21	0.008256	0.407194
Chaihu	Isorhamnetin	MOL000354	21	0.008057	0.411936
Gancao	Licochalcone a	MOL000497	20	0.008444	0.407194

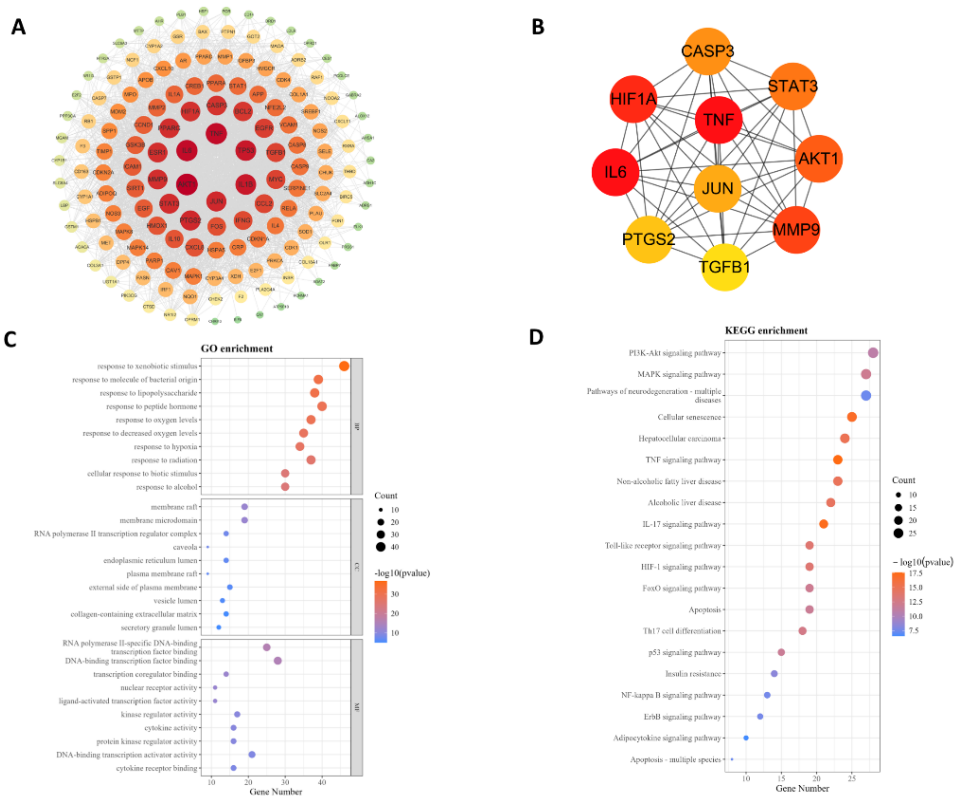


Figure 2. Protein–protein interaction (PPI), Gene Ontology (GO), and Kyoto Encyclopedia of Genes and Genomes (KEGG) enrichment analyses of core targets of Si-Ni-San (SNS) against non-alcoholic fatty liver disease (NAFLD). (A) PPI network of common targets related to both SNS and NAFLD. (B) Top 10 core targets and their associated subnetwork. (C) GO enrichment analysis showing biological processes, molecular functions, and cellular components. The x-axis indicates the number of genes; color represents the *p*-value. (D) KEGG pathway enrichment analysis. The y-axis shows pathways; the x-axis indicates the number of genes; color represents the *p*-value.

3.3. Molecular docking of Si-Ni-San

The top five active components of SNS were docked with STAT3 and NRF2 using AutoDock Vina. Molecular docking studies were conducted under identical conditions, using the reference ligands for STAT3 and NRF2 as positive controls: STAT3 in complex with the inhibitor S3I-201 and NRF2 with the inhibitor ML385. Figure 3 and Table 3 present a comprehensive molecular docking analysis of STAT3 and NRF2 with their respective reference ligands. These results serve as a benchmark for evaluating the binding affinities of the active compounds. The binding affinity (kcal/mol), a key parameter in Vina, reflects the overall quality of ligand–receptor interactions, with more negative values indicating stronger binding. The docking scores of STAT3 and NRF2 with each of the five compounds were all ≤−9 kcal/mol or close to this value, indicating strong binding affinities and the formation of stable complexes between STAT3/NRF2 and each compound. The entry of the compounds into the active pockets was visualized in PyMOL. Representative two-dimensional and 3D images, along with the lowest binding energy values for each protein, are presented in Figure 4. The binding affinity of STAT3 and NRF2 with each of the five compounds is provided in Table 3. The results showed favorable binding affinities between the top five active components and both NRF2 (Figure 4A–E) and STAT3 (Figure 4F–J).

3.4. Si-Ni-San treatment attenuates hepatic steatosis in high-fat diet mice

Non-alcoholic fatty liver disease was induced in mice by HFD administration, and the therapeutic efficacy of SNS was subsequently evaluated. Macroscopic examination of liver morphology showed that NFD mice exhibited reddish and smooth liver surfaces, whereas HFD mice developed hepatomegaly with multifocal yellowish-white plaques. After SNS treatment, the reddish coloration was partially restored (Figure 5A), and both body weight and liver weight exhibited a significant reduction relative to the HFD group ($p < 0.01$; Figure 5B and 5C). Oil Red O staining further showed that SNS treatment reduced hepatic lipid droplet aggregation compared to the HFD group (Figure 5D). Biochemical analyses revealed that HFD treatment significantly elevated serum TC ($p < 0.01$) and TG ($p < 0.05$) levels, which were significantly reduced in SNS-treated mice ($p < 0.05$; Figure 5E and 5F). These results demonstrate that the NAFLD mouse model was successfully established in C57BL/6 mice using a high-fat diet, and that SNS treatment reduced liver weight and ameliorated lipid accumulation in the liver tissue.

3.5. Si-Ni-San ameliorates inflammatory responses associated with non-alcoholic fatty liver disease in mice

To investigate whether the anti-inflammatory effect

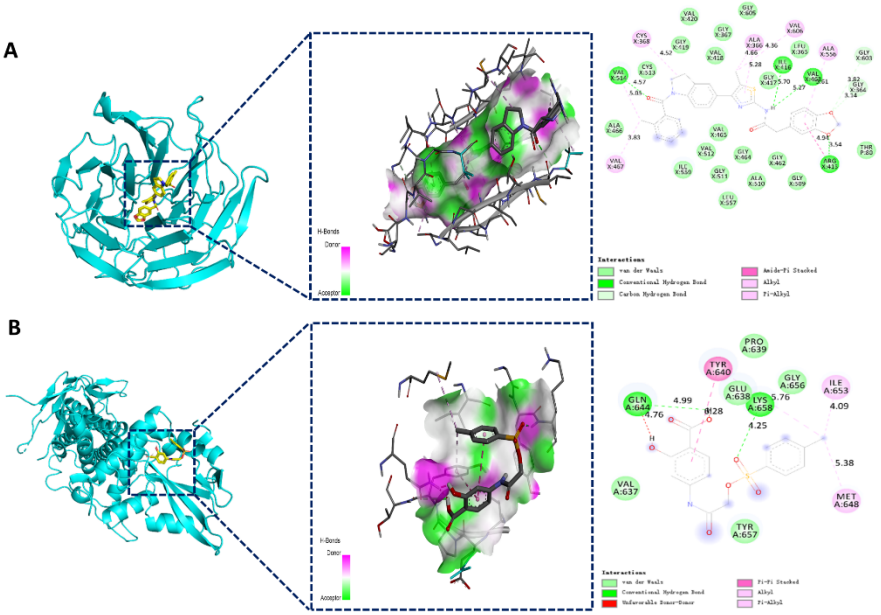


Figure 3. Molecular docking diagrams of STAT3 and NRF2 with reference ligands Docking of NRF2 with ML385. (B) Docking of STAT3 with S3I-201.

Table 3. AutoDock parameters for molecular docking

Receptor	Ligand	Grid center (X, Y, Z)	Grid size (X, Y, Z)	Grid spacing	Exhaustiveness	Binding mode count	Random seed	Best binding affinity
NRF2	Quercetin	10.7, 18.5, 10.4	71.4, 61.1, 58.3	0.375 Å	16	9	29,491	−9.596 kcal/mol
	Kaempferol	10.7, 18.5, 10.4	71.4, 61.1, 58.3	0.375 Å	16	9	19,538	−9.547 kcal/mol
	Luteolin	10.7, 18.5, 10.4	71.4, 61.1, 58.3	0.375 Å	16	9	14,665	−9.378 kcal/mol
	Naringenin	10.7, 18.5, 10.4	71.4, 61.1, 58.3	0.375 Å	16	9	17,996	−8.421 kcal/mol
	Nobiletin	10.7, 18.5, 10.4	71.4, 61.1, 58.3	0.375 Å	16	9	14,986	−8.294 kcal/mol
	ML385	10.7, 18.5, 10.4	71.4, 61.1, 58.3	0.375 Å	16	9	16,841	−11.91kcal/mol
STAT3	Quercetin	14.0, 54.3, −0.3	20.9, 31.7, 23.2	0.375 Å	16	9	10,506	−6.091 kcal/mol
	Kaempferol	14.0, 54.3, −0.3	20.9, 31.7, 23.2	0.375 Å	16	9	5,213	−6.086 kcal/mol
	Luteolin	14.0, 54.3, −0.3	20.9, 31.7, 23.2	0.375 Å	16	9	8,382	−6.386 kcal/mol
	Naringenin	14.0, 54.3, −0.3	20.9, 31.7, 23.2	0.375 Å	16	9	26,351	−6.571 kcal/mol
	Nobiletin	14.0, 54.3, −0.3	20.9, 31.7, 23.2	0.375 Å	16	9	3,589	−5.615 kcal/mol
	S3I-201	14.0, 54.3, −0.3	20.9, 31.7, 23.2	0.375 Å	16	9	17,860	−6.335 kcal/mol

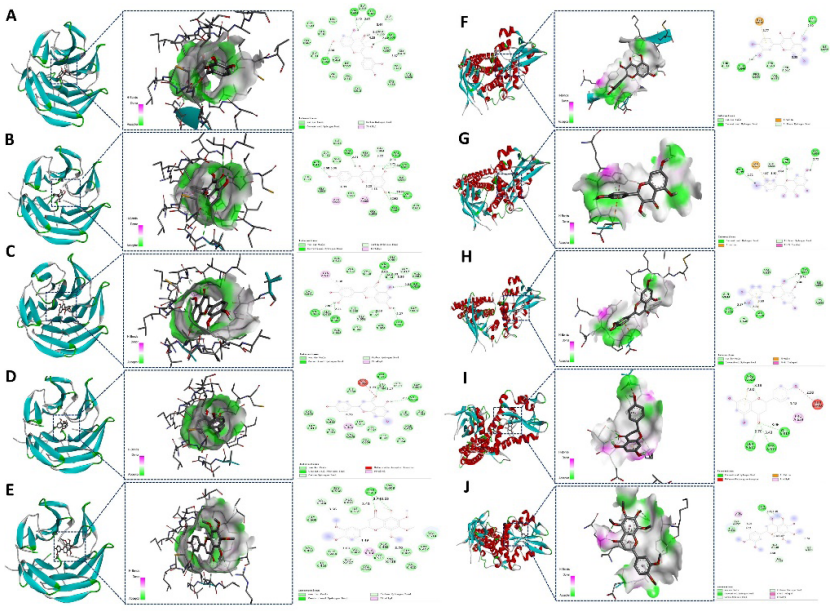


Figure 4. Molecular docking results. Binding conformations between (A) quercetin and NRF2, (B) kaempferol and NRF2, (C) luteolin and NRF2, (D) naringenin and NRF2, (E) nobiletin and NRF2, (F) quercetin and STAT3, (G) kaempferol and STAT3, (H) luteolin and STAT3, (I) naringenin and STAT3, and (J) nobiletin and STAT3.

contributes to the protective role of SNS against NAFLD, we evaluated the inflammatory mediator expression and molecular biological analysis of the JAK2/STAT3 signaling pathway. Our findings demonstrated a significant upregulation of pro-inflammatory cytokines *Tnf*, *Il6*, and *Il1b* in mice fed HFD ($p < 0.001$), whereas SNS treatment markedly suppressed their expression ($p < 0.01$) (Figure 6A–C). Western blot analysis further demonstrated activation of the JAK2/STAT3 pathway in the HFD group, indicated by increased JAK2 and STAT3 phosphorylation ($p < 0.001$). In contrast, SNS treatment reversed this trend (Figure 6D–F).

3.6. Si-Ni-San boosts the antioxidant defense system by activating the Sestrin2/Nrf2 pathway

To elucidate the protective mechanism of SNS against NAFLD, we measured the mRNA expression of the antioxidant factors *Nqo1* and *Hmox1* by qPCR. Additionally, we analyzed key proteins in the Sestrin2/NRF2/HO-1 signaling pathway by Western blot. Compared with the normal control group, the HFD group showed significant downregulation in *Hmox1* ($p < 0.001$) and *Nqo1* ($p < 0.01$) mRNA expression. In contrast, SNS treatment significantly upregulated the expression of both *Hmox1* ($p < 0.001$) and *Nqo1* ($p < 0.05$) (Figure 7A,B). Western blot results demonstrated that HFD feeding markedly decreased Sestrin2 protein expression ($p < 0.001$) and inhibited downstream NRF2 and HO-1 signaling ($p < 0.001$). However, SNS treatment led to a significant reversal, restoring the protein levels of Sestrin2, NRF2, and HO-1, respectively (Figure 7C–F).

4. Discussion

Non-alcoholic fatty liver disease has emerged as a widespread chronic liver disorder on a global scale, presently impacting approximately 25% of the adult population worldwide.[30] SNS, a TCM, is frequently employed as a clinical intervention for chronic liver diseases[31]; however, its specific mechanisms of action remain incompletely elucidated.

Through network pharmacology analysis, we identified 157 overlapping targets between SNS and NAFLD. Notably, three key active compounds—MOL000098 (quercetin), MOL000422 (kaempferol), and MOL000006 (luteolin)—exhibited superior network properties, including the highest number of connecting edges and the most extensive target interactions, suggesting their central role in the therapeutic network. These flavonoids are well documented for their ability to alleviate inflammation, reduce oxidative stress, and regulate immune function,[32] which are known to ameliorate NAFLD pathogenesis.[33–35] For instance, quercetin and kaempferol have been shown to reduce lipid aggregation and mitigate oxidative stress in HepG2 cells.[35,36] These findings underscore the therapeutic potential of flavonoid-rich SNS. Thus, the efficacy of SNS against NAFLD may be attributed to the synergistic actions of these bioactive components along with other constituents. Consistent with this, the *in vivo* experiments demonstrated that SNS treatment effectively alleviated HFD-induced NAFLD in mice, as evidenced by reduced liver weight and hepatic lipid accumulation.

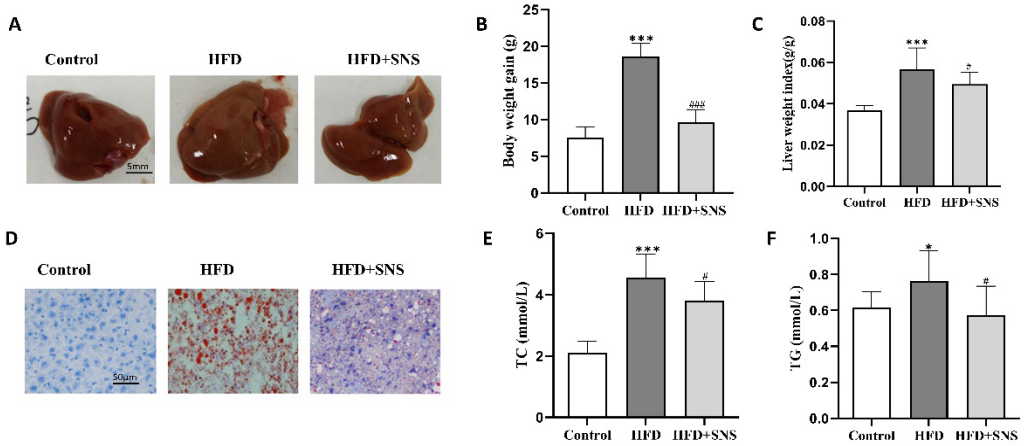


Figure 5. Si-Ni-San (SNS) alleviates hepatic steatosis in NAFLD mice. (A) Representative macroscopic liver images (scale bar: 5 mm). (B) Body weight gain during the experimental period. (C) Liver weight index. (D) Liver Oil Red O staining (scale bar: 50 μm; magnification: ×200). (E–F) Serum levels of TC and TG. Values are expressed as mean ± standard error of the mean ($n = 9$). Compared with the control group, * denotes $p < 0.05$, *** denotes $p < 0.001$; compared with the HFD group, $^{\#}$denotes $p < 0.05$, $^{\#\#}$ denotes $p < 0.01$, $^{\#\#\#}$ denotes $p < 0.001$.
Abbreviations: HFD: High-fat diet; NAFLD: Non-alcoholic fatty liver disease; TC: Total cholesterol; TG: Triglyceride.

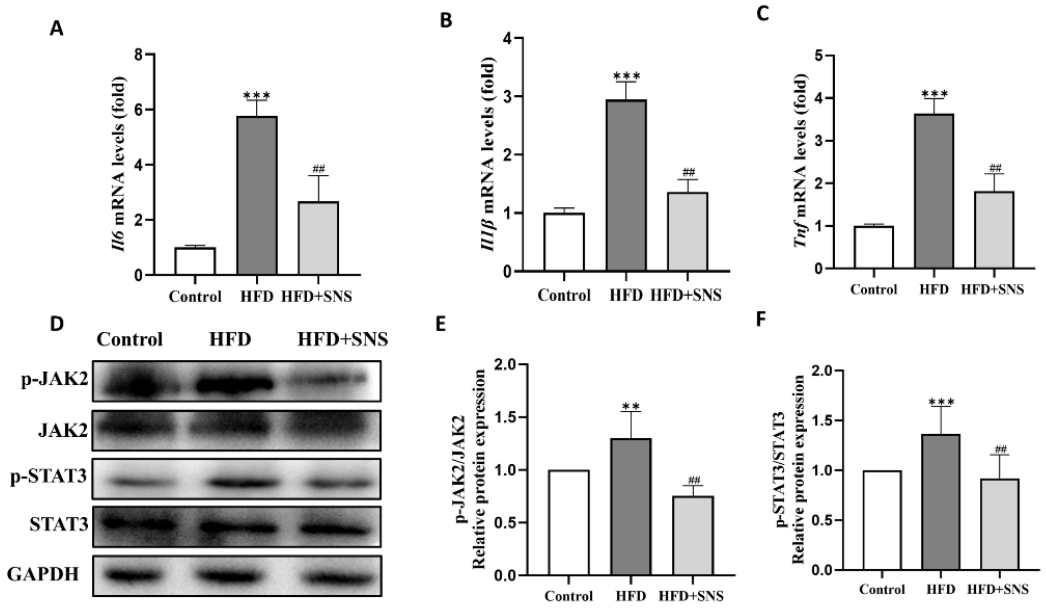


Figure 6. Si-Ni-San (SNS) mitigates inflammatory responses in non-alcoholic fatty liver disease mice. The gene expression of (A) *Il6*, (B) *Il1b*, and (C) *Tnf*. (D) Representative Western blot results of related proteins. Quantitative analysis of (E) p-JAK2 and (F) p-STAT3 protein levels. Results were exhibited as mean ± standard error of the mean ($n = 4$). Compared with the control group,** denotes $p < 0.01$, *** denotes $p < 0.001$; compared with the HFD group, ## denotes $p < 0.01$.
Abbreviation: HFD: High-fat diet.

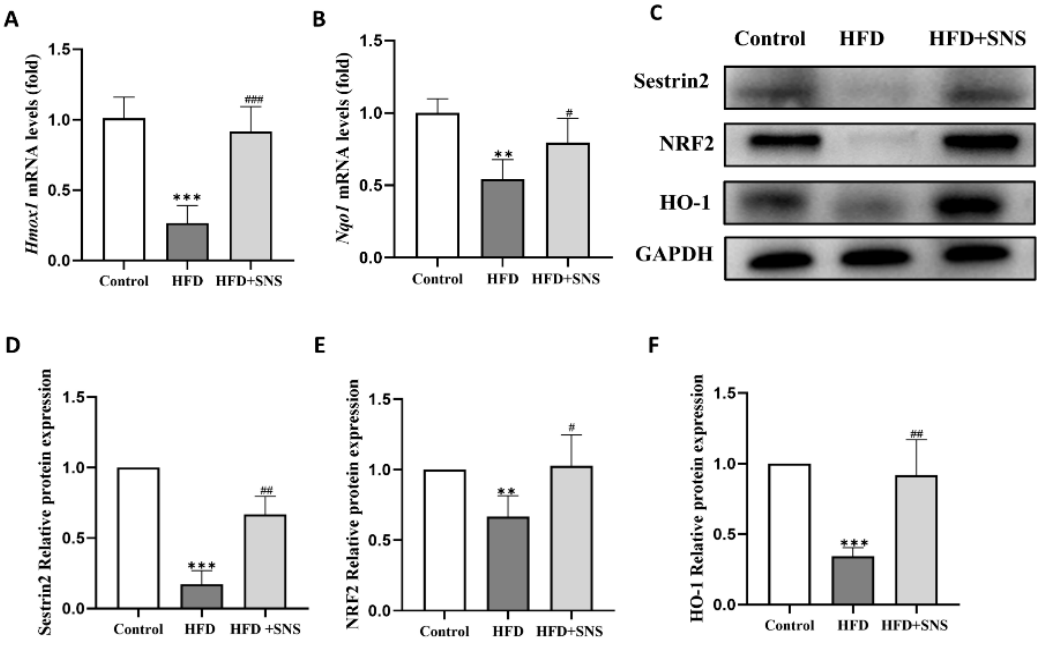


Figure 7. Si-Ni-San (SNS) enhances antioxidant capacity in non-alcoholic fatty liver disease mice. mRNA expression levels of (A) *Hmox1* and (B) *Nqo1*. (C) Representative Western blot images of proteins in the Sestrin2/NRF2/HO-1 signaling pathway. Quantitative analysis of (D) Sestrin2, (E) NRF2, and (F) HO-1 protein expression. Values are expressed as mean ± standard error of the mean ($n = 4$). Compared with the control group, ** denotes $p < 0.01$, *** denotes $p < 0.001$; compared with the high-fat diet (HFD) group, # denotes $p < 0.05$, ## denotes $p < 0.01$, ### *denotes* $p < 0.001$.

Research indicates that pro-inflammatory cytokines such as IL-1β, TNF-α, IL-6, IL-8, and COX-2 play a pivotal role in the progression of chronic inflammatory diseases.[36] By constructing the PPI network to visualize and analyze 157 targets, the top 10 hub targets were screened based on degree values, primarily including IL-6, TNF, HIF-1α, MMP-9, AKT1, STAT3, Caspase-3, JUN, PTGS2, and TGF-β1. Notably, the pro-inflammatory factors IL-6, TNF, AKT1, and STAT3 may represent critical therapeutic targets for SNS in NAFLD. TNF-α and IL-6 serve as core upstream activators of the JAK2/STAT3 pathway. Specifically, IL-6 binding to its receptor (IL-6R) triggers JAK2 phosphorylation via a gp130-dependent mechanism, which, in turn, induces STAT3 phosphorylation. The p-STAT3 then translocates into the nucleus to modulate the transcription of target genes (e.g., pro-inflammatory genes *IL1β* and *IL6*), thereby amplifying the inflammatory response.[37] TNF-α and the JAK2/STAT3 pathway form a bidirectional regulatory network: TNF-α acts as both an activator and a downstream effector of the JAK2/STAT3 pathway, while JAK2/STAT3 activation amplifies TNF-α-mediated inflammatory responses.[38] Compounds like ginkgetin inhibit the phosphorylation of JAK2 and STAT3, concurrently attenuating inflammatory mediators such as IL-6 and TNF-α, thereby improving histological outcomes and liver metabolic function.[39] Zhang *et al.*[40] demonstrated that quercetin alleviates hepatic injury by directly suppressing the IL-6/STAT3 signaling pathway, leading to significant downregulation of inflammatory cytokines (including *IL-6* and *IL-1β*). Similar to the above findings, PPI network analysis revealed that IL-6, TNF-α, IL-1β, and STAT3 are key targets of SNS in the treatment of NAFLD. Molecular docking results further confirmed a strong binding affinity between STAT3 and the active components of SNS. The present *in vivo* experiments validated the targets identified by network pharmacology, demonstrating that SNS treatment significantly downregulated the mRNA levels of *Il1b*, *Il6*, and *Tnf* in the livers of NAFLD mice, while markedly reducing the protein expression of p-JAK2/JAK2 and p-STAT3/STAT3. These results indicate that SNS inhibits the inflammatory response in NAFLD mice by suppressing the JAK2/STAT3 signaling pathway.

Inflammation and oxidative stress exhibit a reciprocal relationship, in which each process exacerbates the other, leading to progressive amplification during NAFLD pathogenesis.[41,42] During inflammatory responses, infiltrating immune cells (e.g., neutrophils and macrophages) intrinsically release reactive oxygen species (ROS), thereby further elevating oxidative stress levels.[43] Excessive ROS production subsequently activates inflammatory pathways and triggers the release of pro-inflammatory cytokines (including TNF-α and IL-6), ultimately resulting in tissue damage.[44] The NRF2 pathway serves as the core of antioxidant defense, and its activation can effectively suppress inflammatory responses.[45] Sestrin2, an endogenous antioxidant protein, inhibits KEAP1, promoting the release of NRF2 from KEAP1 binding, enabling NRF2 nuclear translocation and the subsequent activation of downstream antioxidant genes (including *Hmox1*), thereby augmenting cellular antioxidant capacity.[25] The activation of HO-1 further enhances free radical scavenging capacity, thereby alleviating lipid peroxidation and cellular damage.[46] Tian *et al.*[47] demonstrated that Tan IIA upregulates Sestrin2 expression and activates HO-1, significantly ameliorating hepatic pathological changes and protecting against sepsis-induced liver injury. In a hepatic fibrosis model, Liu *et al.*[48] further revealed that hiHep-EVs alleviate fibrosis by activating the NRF2/HO-1 signaling pathway, which upregulates NQO1 and HO-1 protein expression, reduces hepatic stellate cell activation, and decreases collagen deposition. This network pharmacology study predicted that NRF2 is a key target of SNS in the treatment of NAFLD. *In vivo* validation experiments demonstrated that SNS treatment upregulated mRNA expression of antioxidant factors (*Nqo1* and *Hmox1*) and protein levels of key pathway components (Sestrin2, NRF2, and HO-1) in NAFLD mice. These findings indicate that SNS ameliorates NAFLD progression, potentially by enhancing the endogenous antioxidant function of the Sestrin2/NRF2/HO-1 pathway.

5. Conclusion

In conclusion, our study combined network pharmacology with experimental validation to systematically explore the mechanisms through which SNS ameliorates NAFLD. The results suggest that SNS may activate the Sestrin2/NRF2/HO-1 signaling pathway to enhance antioxidant ability, while concurrently inhibiting the JAK2/STAT3 pathway to alleviate inflammatory injury. Nevertheless, several limitations persist, particularly concerning the precise regulatory mechanisms by which SNS modulates these pathways. Future research should focus on designing *in vitro* experiments, particularly employing free fatty acid-induced lipid accumulation models in AML-12 or HepG2 hepatocytes, alongside SNS intervention. This methodology seeks to ascertain whether SNS exerts direct effects on the relevant targets within hepatocytes. However, the study was not designed to dissect the individual contributions of specific compounds; this remains beyond the scope of the current phase of research, which focused on formula-level validation. In follow-up studies, we plan to use individual pure compounds (e.g., quercetin, kaempferol) in parallel animal or cell experiments, and to employ a

component-knockout strategy (i.e., comparing the full SNS formula with a version lacking a specific compound) to directly evaluate the functional contribution of each key constituent.

Acknowledgments

None.

Funding

The present study was supported by the Henan Province Scientific and Technology Research Project (Grant No. 262102310193) and the College Student Innovation and Entrepreneurship Training Program of Henan Province (Grant No. S202510464081).

Conflict of interest

The authors declare no competing interests regarding the publication of this manuscript.

Author contributions

Conceptualization: Jingxia Du
Formal analysis: Bowen Yang, Yishu Wang, Cancan Guo
Investigation: Yue Hu, Tingting Wang, Chengyao Xiao, Bowen Yang, Yishu Wang, Yunfei Li
*Methodology:*Yue Hu
Writing–original draft: Yue Hu
Writing–review & editing: Jingxia Du
All of the authors have approved the final manuscript.

Ethics approval and consent to participate

This study was approved by the Animal Care and Ethics Committee of Henan University of Science and Technology (license number: HAUST-025-M0221052) and in accordance with the Guide for the Care and Use of Laboratory Animals of the National Institutes of Health Guidelines.

Consent for publication

Not applicable.

Availability of data and materials

The original contributions presented in the study are included in the article and the Supplementary File. Further inquiries can be directed to the corresponding author.

References

1. Saiman Y, Duarte-Rojo A, Rinella ME. Fatty Liver Disease: Diagnosis and Stratification. *Annu Rev Med*. 2022;73(1):529–544.

   doi: 10.1146/annurev-med-042220-020407

2. Lee YA, Friedman SL. Inflammatory and fibrotic mechanisms in NAFLD-Implications for new treatment strategies. *J Intern Med*. 2022;291(1):11–31.

   doi: 10.1111/joim.13380

3. Paternostro R, Trauner M. Current treatment of non-alcoholic fatty liver disease. *J Intern Med*. 2022;292(2):190–204.

   doi: 10.1111/joim.13531

4. Allameh A, Niayesh-Mehr R, Aliarab A, *et al*. Oxidative Stress in Liver Pathophysiology and Disease. *Antioxidants*. 2023;12(9):1653.

   doi: 10.3390/antiox12091653

5. Chen P, Yao L, Yuan M, *et al*. Mitochondrial dysfunction: A promising therapeutic target for liver diseases. *Genes Dis*. 2024;11(3):101115.

   doi: 10.1016/j.gendis.2023.101115

6. Liang C, Li J, Tian B, *et al*. Foresight regarding drug candidates acting on the succinate-GPR91 signalling pathway for non-alcoholic steatohepatitis (NASH) treatment. *Biomed Pharmacother*. 2021;144:112298.

   doi: 10.1016/j.biopha.2021.112298

7. Fredrickson G, Barrow F, Dietsche K, *et al*. Exercise of high intensity ameliorates hepatic inflammation and the progression of NASH. *Mol Metab*. 2021;53:101270.

   doi: 10.1016/j.molmet.2021.101270

8. Bence KK, Birnbaum MJ. Metabolic drivers of non-alcoholic fatty liver disease. *Mol Metab*. 2021;50:101143.

   doi: 10.1016/j.molmet.2020.101143

9. Ramai D, Facciorusso A, Vigandt E, *et al*. Progressive Liver Fibrosis in Non-Alcoholic Fatty Liver Disease. *Cells*. 2021;10(12):3401.

   doi: 10.3390/cells10123401

10. Wang Y, Yi H, Sun W, *et al*. Comparative Efficacy of Drug Interventions on NAFLD Over 24 Weeks: A Traditional and Network Meta-Analysis of Randomized Controlled Trials. *Drugs*. 2024;84(4):425–439.

    doi: 10.1007/s40265-024-02015-6

11. Lan T, Geng X-J, Zhang S-J, *et al*. Si-Ni-San inhibits hepatic Fasn expression and lipid accumulation in MAFLD mice through AMPK/p300/SREBP-1c axis. *Phytomedicine*. 2024;123:155209.

    doi: 10.1016/j.phymed.2023.155209

12. Zhu F, Ding Y, Chen L, *et al*. Regulatory effects of Sini-San on bile acid homeostasis in the enterohepatic circulation of mice with liver fibrosis. *Chin Med*. 2025;20(1):186.

    doi: 10.1186/s13020-025-01252-5

13. Liu Z, Shang Q, Cheng J, *et al*. Mechanistic study of a

triterpenoid-enriched fraction derived from Cynomorium songaricum against NAFLD: An integrative elucidation. *Phytomedicine*. 2025;142:156782.

doi: 10.1016/j.phymed.2025.156782

14. Jiao X, Jin X, Ma Y, *et al*. A comprehensive application: Molecular docking and network pharmacology for the prediction of bioactive constituents and elucidation of mechanisms of action in component-based Chinese medicine. *Comput Biol Chem*. 2021;90:107402.

doi: 10.1016/j.compbiolchem.2020.107402

15. Marinello PC, Cella PS, Testa MTJ, *et al*. Creatine supplementation protects against diet-induced non-alcoholic fatty liver but exacerbates alcoholic fatty liver. *Life Sci*. 2022;310: 121064.

doi: 10.1016/j.lfs.2022.121064

16. Li S, Guo L. The role of Sirtuin 2 in liver - An extensive and complex biological process. *Life Sci*. 2024; 339:122431.

doi: 10.1016/j.lfs.2024.122431

17. Gu Y, Duan S, Ding M *et al*. Saikosaponin D attenuates metabolic associated fatty liver disease by coordinately tuning PPARα and INSIG/SREBP1c pathway. *Phytomedicine*. 2022;103: 154219.

doi: 10.1016/j.phymed.2022.154219

18. Philips RL, Wang Y, Cheon H, *et al*. The JAK-STAT pathway at 30: Much learned, much more to do. *Cell*. 2022;185(21):3857–3876.

doi: 10.1016/j.cell.2022.09.023

19. Xue C, Yao Q, Gu X, *et al*. Evolving cognition of the JAK-STAT signaling pathway: autoimmune disorders and cancer. *Signal Transduct Target Ther*. 2023;8(1):204.

doi: 10.1038/s41392-023-01468-7

20. Roskoski R. Janus kinase (JAK) inhibitors in the treatment of neoplastic and inflammatory disorders. *Pharmacol Res*. 2022;183:106362.

doi: 10.1016/j.phrs.2022.106362

21. Wong GL, Manore SG, Doheny DL, *et al*. STAT family of transcription factors in breast cancer: Pathogenesis and therapeutic opportunities and challenges. *Semin Cancer Biol*. 2022;86:84–106.

doi: 10.1016/j.semcancer.2022.08.003

22. Wu Y, Zhang J, Li G, *et al*. Exosomal miR-320d promotes angiogenesis and colorectal cancer metastasis via targeting GNAI1 to affect the JAK2/STAT3 signaling pathway. *Cell Death Dis*. 2024;15(12):913.

doi: 10.1038/s41419-024-07297-y

23. Sun Y, Tong H, Chu X, *et al*. Notch1 regulates hepatic thrombopoietin production. *Blood*. 2024;143(26):2778–2790.

doi: 10.1182/blood.2023023559

24. Ding W, Zhao Z, Zheng Y, *et al*. Exposure to short-chain chlorinated paraffins induces astrocyte activation via JAK2/STAT3 signaling pathway. *Ecotoxicol Environ Saf*. 2022;248: 114268.

doi: 10.1016/j.ecoenv.2022.114268

25. Zhang L, Ding K, Liao S-S, *et al*. Sestrin2 reduces ferroptosis via the Keap1/Nrf2 signaling pathway after intestinal ischemia-reperfusion. *Free Radic Biol Med*. 2024;214:115–128.

doi: 10.1016/j.freeradbiomed.2024.02.003

26. Lu C, Jiang Y, Xu W, *et al*. Sestrin2: multifaceted functions, molecular basis, and its implications in liver diseases. *Cell Death Dis*. 2023;14(2):160.

doi: 10.1038/s41419-023-05669-4

27. Li W, Yang S, Zhao Y, *et al*. Ginseng-derived nanoparticles alleviate alcohol-induced liver injury by activating the Nrf2/HO-1 signalling pathway and inhibiting the NF-κB signalling pathway in vitro and in vivo. *Phytomedicine*. 2024;127:155428.

doi: 10.1016/j.phymed.2024.155428

28. Wang Y, Fu X, Zeng L, *et al*. Activation of Nrf2/HO-1 signaling pathway exacerbates cholestatic liver injury. *Commun Biol*. 2024;7(1):621.

doi: 10.1038/s42003-024-06243-0

29. Yang H, Zhang P, Wang Q, *et al*. The research development of STAT3 in hepatic ischemia-reperfusion injury. *Front Immunol*. 2023;14:1066222.

doi: 10.3389/fimmu.2023.1066222

30. Targher G, Byrne CD, Tilg H. NAFLD and increased risk of cardiovascular disease: clinical associations, pathophysiological mechanisms and pharmacological implications. *Gut*. 2020; 69(9):1691–1705.

doi: 10.1136/gutjnl-2020-320622

31. Zhang N, Liu T, Wang J, *et al*. Si-Ni-San Reduces Hepatic Lipid Deposition in Rats with Metabolic Associated Fatty Liver Disease by AMPK/SIRT1 Pathway. *Drug Des Devel Ther*. 2023;17:3047–3060.

doi: 10.2147/DDDT.S417378

32. Jomova K, Alomar SY, Valko R, *et al*. Flavonoids and their role in oxidative stress, inflammation, and human diseases. *Chem Biol Interact*. 2025;413:111489.

doi: 10.1016/j.cbi.2025.111489

33. Li S, Wang S, Zhang L, *et al*. Research progress on pharmacokinetics, anti-inflammatory and immunomodulatory effects of kaempferol. *Int Immunopharmacol*. 2025;152:114387.

doi: 10.1016/j.intimp.2025.114387

34. Shi Z, Zhang C, Lei H, *et al*. Structural Insights into Amelioration Effects of Quercetin and Its Glycoside Derivatives on NAFLD in Mice by Modulating the Gut Microbiota and Host Metabolism. *J Agric Food Chem*. 2022;70(46):14732–14743.

doi: 10.1021/acs.jafc.2c06212

35. Yao C, Dai S, Wang C, *et al*. Luteolin as a potential hepatoprotective drug: Molecular mechanisms and treatment strategies. *Biomed Pharmacother*. 2023;167:115464.

doi: 10.1016/j.biopha.2023.115464

36. Ren L, Wang R, Wang Y, *et al*. Exploring the effect and mechanism of Hippophae rhamnoides L. triterpenoid acids on improving NAFLD based on network pharmacology and experimental validation in vivo and in vitro. *J Ethnopharmacol*. 2024;335:118657.

doi: 10.1016/j.jep.2024.118657

37. Baumgartner F, Bamopoulos SA, Faletti L, *et al*. Activation of gp130 signaling in T cells drives TH17-mediated multi-organ autoimmunity. *Sci Signal*. 2024;17(824):eadc9662.

doi: 10.1126/scisignal.adc9662

38. Tao Y, Liu J, Li M, *et al*. Abelmoschus manihot (L.) medik. seeds alleviate rheumatoid arthritis by modulating JAK2/STAT3 signaling pathway. *J Ethnopharmacol*. 2024;325:117641.

doi: 10.1016/j.jep.2023.117641

39. Wang C, Bai Y, Li T, *et al*. Ginkgetin exhibits antifibrotic effects by inducing hepatic stellate cell apoptosis via STAT1 activation. *Phytother Res*. 2024;38(3):1367–1380.

doi: 10.1002/ptr.8106

40. Zhang H, Shi H, Li X, *et al*. Quercetin alleviates LPS/iE-DAP-induced liver injury by suppressing ferroptosis via regulating ferritinophagy and intracellular iron efflux. *Redox Biol*. 2025;81:103557.

doi: 10.1016/j.redox.2025.103557

41. Barrea L, Verde L, Savastano S, *et al*. Adherence to Mediterranean Diet: Any Association with NAFLD? *Antioxidants*. 2023;12 (7):1318.

doi: 10.3390/antiox12071318

42. Lai W, Zhang J, Sun J, *et al*. Oxidative stress in alcoholic liver disease, focusing on proteins, nucleic acids, and lipids: A review. *Int J Biol Macromol*. 2024;278:134809.

doi: 10.1016/j.ijbiomac.2024.134809

43. Park MN, Rahman MA, Rahman MH, *et al*. Potential Therapeutic Implication of Herbal Medicine in Mitochondria-Mediated Oxidative Stress-Related Liver Diseases. *Antioxidants*. 2022;11(10):2041.

doi: 10.3390/antiox11102041

44. Arellano-García L, Trepiana J, Martínez JA, *et al*. Beneficial Effects of Viable and Heat-Inactivated Lactobacillus rhamnosus GG Administration on Oxidative Stress and Inflammation in Diet-Induced NAFLD in Rats. *Antioxidants*. 2023;12(3):717.

doi: 10.3390/antiox12030717

45. O'Rourke SA, Shanley LC, Dunne A. The Nrf2-HO-1 system and inflammaging. *Front Immunol*. 2024;15:1457010.

doi: 10.3389/fimmu.2024.1457010

46. Shu Y, Wu X, Zhang D, Jiang S, *et al*. Exploring the Mechanisms of Iron Overload-Induced Liver Injury in Rats Based on Transcriptomics and Proteomics. *Biology*. 2025;14(1): 81.

doi: 10.3390/biology14010081

47. Tian W, Song P, Zang J, *et al*. Tanshinone IIA, a component of Salvia miltiorrhiza Bunge, attenuated sepsis-induced liver injury via the SIRT1/Sestrin2/HO-1 signaling pathway. *J Ethnopharmacol*. 2025;340:119169.

doi: 10.1016/j.jep.2024.119169

48. Liu W, Wu J, Cao H, *et al*. Human-Induced Hepatocytes-Derived Extracellular Vesicles Ameliorated Liver Fibrosis in Mice Via Suppression of TGF-β1/Smad Signaling and Activation of Nrf2/HO-1 Signaling. *Stem Cells Dev*. 2023;32(19-20):638–651.

doi: 10.1089/scd.2023.0110